



Influence of soil-structure interaction (SSI) on optimal design of passive damping devices

Ersin Aydin^a, Baki Ozturk^b, Aleksandra Bogdanovic^c, Ehsan Noroozinejad Farsangi^{d,*}

^a Department of Civil Engineering, Nigde Ömer Halisdemir University, Nigde, Turkey

^b Department of Civil Engineering, Hacettepe University, Ankara, Turkey

^c Institute of Earthquake Engineering and Engineering Seismology, Skopje, N. Macedonia

^d Faculty of Civil and Surveying Engineering, Graduate University of Advanced Technology, Kerman, Iran

ARTICLE INFO

Keywords:

Soil-structure interaction
Viscous dampers
Optimal dampers
Earthquake response
Sandy soil

ABSTRACT

Recently, the interest in research for optimization of viscous dampers in design of buildings has been increasing. In this study, the effect of soil-structure interaction has been taken into account for the purpose of optimal design of viscous dampers. A damper optimization method based on a target damping ratio and interstorey drift ratio found in literature has been adapted for a building structure model considering different types of sandy soils. While passive constraints have been taken as upper and lower limits of each damper, active constraints have been considered as a target damping ratio in terms of damping coefficients. The proposed algorithm includes time history analyses that test the designer's optimal design. Interstorey drift ratios under design earthquakes have been checked at each design step. The first and second mode responses have been considered separately. According to the results obtained from this study, the negative impact of sandy soils on the dynamic behavior of superstructures can be overcome by optimal placement of dampers in buildings. The results of the analyses have shown that soil effects should be taken into account in solving damper optimization problems.

1. Introduction

In classical structural design, it is frequently accepted that a foundation is simply related to a rigid rock exposed to lateral unidirectional acceleration, while soil-structure interaction (SSI) is generally ignored in design of earthquake-resistant structures. In recent years, many design codes such as Eurocode8 [20] and ASCE/SEI 7 [2] have begun to consider design guidelines that include the SSI effects. Presently, passive dampers are widely used for vibration control of earthquake-resistant buildings. However, studies aimed at structural passive vibration control including SSI effects are quite limited. In this study, the influence of SSI on optimal design of viscous dampers has been examined. The corresponding results of the analyses are discussed in this paper.

It is well known that soil-structure interaction starts as early as in the construction phase. The stresses and deformations that occur in a newly built building affect the ground on which the building lies, while on the other hand, ground movements affect the building. After a certain period of time, these movements become balanced. It is obvious that the extent of interaction is very important, especially for highly compressible soil structures. The flexibility of soil causes the foundations to settle and rotate under loads. The relative stiffness of a

structure, foundation, and ground determines the behavior of the SSI system.

Early researches related to SSI are the works of Chameski [17], Morris [38], Lee and Harrison [34], Lee and Brown [33]. They cover analytical models of interaction problems in the case of frames with isolated footings. Moreover, they provide an overview of raft foundations as well as problems of interaction with combined footings. Experimental results are tried to be verified numerically by analyses performed in both the time and frequency domain. Stewart et al. [46,47] observed a high correlation between the soil stiffness ratio and the lengthening ratio of the structure's period resulting from the flexibility of the foundation and the structure. Kitada et al. [32], Yano et al. [59,60], and Kitada and Iguchi [31] examined the SSI problem related to nuclear power plants in situ and in laboratory. Muria-Vila et al. [39] showed that SSI has an influence on the stiffness and the frequencies of a structure. Ingle and Chore [26] noted that SSI must be considered in the case of a frame structure system founded on a pile structure and pointed out the necessity of interaction analysis including coupled and uncoupled approaches to 3D frame structures with pile foundations. To evaluate and explain the effect of SSI on structures, experimental and in situ tests were also conducted. Ptilakis et al. [42] studied SSI by

* Corresponding author.

E-mail address: noroozinejad@kgut.ac.ir (E. Noroozinejad Farsangi).

<https://doi.org/10.1016/j.istruc.2020.09.028>

Received 17 February 2020; Received in revised form 10 September 2020; Accepted 11 September 2020

2352-0124/ © 2020 Institution of Structural Engineers. Published by Elsevier Ltd. All rights reserved.

performing a shake table test designed to prove the ability of simulation of these effects. El Ganainy and El Naggar [19] showed that, under cyclic loading, a shear hinge connected to an elastic frame element in series, can simulate rocking and lateral behavior of shallow foundations well. The positive effects of SSI were considered by Guzman [23], who studied the problem of the contact between a strap beam and a bearing stratum. These positive effects led to relieving the pressure of the soil and preventing the failure of the strap beam. The FEMA-440 recommendations for the SSI effects were studied by Khoshnoudian and Behmanesh [29].

Li et al. [35] conducted shake table tests including SSI on two adjacent 12-storey reinforced concrete frame models lying on 3x3 group piles. Trombetta et al. [51,52] and Mason et al. [37] investigated the effects of SSI by using physical models in centrifuge tests. Xiong et al. [56] showed that the fundamental period of a structure can be estimated perfectly by using the Dunkerley's equation for SSI. This formula can be a useful reference for future seismic codes considering the fundamental period of a structure in the evaluation of SSI. Lu et al. [36] proposed a new design factor RF to capture the strength reduction in single-degree-of-freedom structures due to combination of SSI and structural yielding. Also, the new site and interaction-dependent modification factor RM was presented in order to take into account multi-degree-of-freedom systems. The RF and RM factors were integrated into a novel performance-based design method for site and interaction-dependent seismic design of flexibility-based structures. Arboleda et al. [4] recommended consideration of the SSI effects in tall building models to avoid underestimation of earthquake-induced direct losses. In general, the addition of SSI effects to the response of tall buildings triggered larger losses compared to other fixed-base structures.

In recent years, seismic control of structures has emerged as a very popular area of research, especially in the domain of dynamic effects such as earthquakes and winds. Structural systems with viscous dampers, as elements of passive control, have also been widely used. Constantinou and Tadjbakhsh [18] conducted a study that used first storey damping for decreasing the seismic behaviour of multi-storey shear frames. Ashour and Hanson [5] proposed a method for optimal placement of visco-elastic dampers regarding seismic excitation. Zhang et al. [62] performed an assessment of the impact of additional visco-elastic dampers on lowering the earthquake response of multi-storey steel frame structures. To find the optimal placement of a viscous damper, an optimization method for a linear conservative mechanical system based on the energy criterion [22] is presented. It is shown that adding visco-elastic dampers from the bottom to half of the total floors of a building is sufficient for the seismic response of shear-buildings with uniform storey stiffness [24]. A design method was developed to find the optimal configuration of viscous dampers in a structure by Zhang and Soong [61]. Cao and Mlejnek [13] introduced a perturbation method based on the finite element approach. Tsuji and Nakamura [53] developed a procedure to find the optimal design in terms of storey stiffness and damping coefficients of dampers for an elastic 2D shear building. A controllability index was minimized for optimal damper problems by Zhang and Soong [61] and Shukla and Datta [45].

Regarding the development of an optimal damper concept, several studies have been performed and presented. The optimum placement of these technological devices in buildings has been the focus of research in the earthquake engineering community [1,7,9,12,15,16,21,25,28]. In literature, almost all studies related to damper problems do not consider the soil effect. Even though it is well known that the soil effect is an important issue regarding earthquake behavior of structures, there is a limited number of studies on optimal passive structural control considering SSI. However, there is a pioneer study [49] on an SSI model in which both viscous damper and tuned mass damper have been used. Furthermore, the soil effect has been considered in modeling the structural response by using the formulations given by Takewaki [50]. There have been studies that have generally been focused on optimal control by use of a tuned mass damper [10,27,30,40,41]. In addition,

few studies (i.e. Xuefei et al. [57,58]) considering the SSI in buildings with viscoelastic dampers. Sarcheshmehpour et al. [43] studied the optimum placement of supplemental viscous dampers for seismic rehabilitation of steel frames considering SSI.

In general, it has been proven that the interaction between the buildings and the ground has serious effects on structural behavior in the design of earthquake-resistant buildings. Furthermore, it is not possible to consider a building acting independently of the ground or an infrastructure acting independently of a superstructure, therefore the SSI effects should be included in solving this design problem and determining more accurately the design principles for viscous dampers. Accordingly, the objective of this study has been to investigate the effect of sandy soils on the optimal design of viscous dampers in building structures. The optimal design of viscous dampers for loose, moderately dense, dense sandy soil conditions and rigid conditions has been studied and the results have been compared. In many previous studies on damper optimization, the ground effect has been neglected and the design principles have been established by assuming a rigid ground. To overcome this shortcoming, in this study, the structure and the sandy soil have been modeled together, while the optimum damper design has been investigated on a more realistic model exposed to earthquake effects. Moreover, this study has shown that structural behavior in poor soil conditions can be improved by adding dampers only, without any soil improvement.

2. Formulation of soil-structure interaction problem

An n -storey shear building with SSI is modelled as shown in Fig. 1. The model building is exposed to the lateral earthquake loads. Assume that u , M , K , C and r denote the generalized displacement vector, mass matrix, stiffness matrix, damping matrix of structure and the influence vector, respectively. The influence vector is defined as $r = \{0, \dots, 0, 1, 0\}^T$. The elements of M and K matrices are known. The structural damping matrix is chosen as proportional to mass. The differential equation of motion in terms of time is given as follows:

$$\mathbf{M}\ddot{u} + \mathbf{C}\dot{u} + \mathbf{K}u = -\mathbf{M}r\ddot{u}_g \quad (1)$$

The set $u = \{u_1, \dots, u_n, u_s, \theta_R\}^T$ is treated here as the generalized displacements vector. While k_s and k_R represent the stiffness of swaying and rocking springs, c_s and c_R denote the damping coefficients of the swaying and rocking dashpots. The total mass matrix of the SSI system may be expressed as

$$\mathbf{M} = \begin{bmatrix} \mathbf{M}_B & \mathbf{M}_{BS} & \mathbf{M}_{BR} \\ E_1 & E_2 & \\ \text{Sym.} & E_3 & \end{bmatrix} \quad (2)$$

where \mathbf{M} is the mass matrix of SSI, \mathbf{M}_B is the mass matrix of upper structure, \mathbf{M}_{BS} and \mathbf{M}_{BR} are mass matrices including the linear swaying and rocking spring. E_1 , E_2 , and E_3 given in Eq. (2) can be calculated as follows

$$E_1 = m_0 + m_1 + \dots + m_n \quad (3)$$

$$E_2 = m_1 H_1 + m_2 H_2 + \dots + m_n H_n \quad (4)$$

$$E_3 = m_1 H_1^2 + m_2 H_2^2 + \dots + m_n H_n^2 + I_{R0} + I_{R1} + I_{R2} + \dots + I_{Rn} \quad (5)$$

H_i , m_i and I_{Ri} ($i = 1, \dots, n$) denote the height of the i th floor from the ground surface, i th storey mass and mass moment of inertia of i th storey, respectively. If Equations (3), (4) and (5) are put into Eq. (2), the system mass matrix is obtained as in Equation (6).

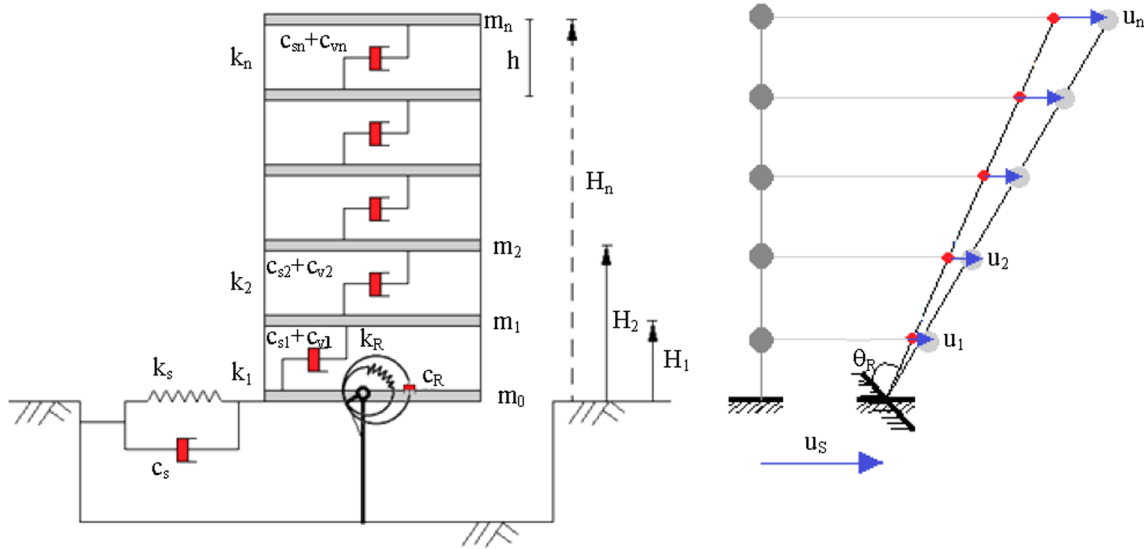


Fig. 1. Shear-building soil-structure model and its deformation.

$$\mathbf{M} = \begin{bmatrix} m_1 & 0 & 0 & 0 & 0 & m_1 & m_1 H_1 \\ 0 & m_2 & 0 & 0 & 0 & m_2 & m_2 H_2 \\ 0 & 0 & \cdot & 0 & 0 & \cdot & \cdot \\ 0 & 0 & 0 & \cdot & 0 & \cdot & \cdot \\ 0 & 0 & 0 & 0 & m_n & m_n & m_n H_n \\ m_1 & m_2 & \cdot & \cdot & m_n & \sum_{i=1}^n m_i & \sum_{i=1}^n m_i H_i \\ m_1 H_1 & m_2 H_2 & \cdot & \cdot & m_n H_n & \sum_{i=1}^n m_i H_i & \sum_{i=1}^n m_i H_i^2 + \sum_{i=0}^n I_{Ri} \end{bmatrix} \quad (6)$$

The stiffness matrix of the SSI system is given as follow

$$\mathbf{K} = \mathbf{K}_B + \mathbf{K}_S + \mathbf{K}_R \quad (7)$$

where \mathbf{K} is the total system stiffness matrix, \mathbf{K}_B is the superstructure stiffness matrix; \mathbf{K}_S and \mathbf{K}_R are the ground linear stiffness matrices including only swaying (k_s) and rocking (k_R) springs, respectively. The ground stiffness parameters and system stiffness matrix are known as follows

$$\mathbf{K} = \begin{bmatrix} k_{s1} + k_{s2} & -k_{s2} & 0 & 0 & 0 & 0 & 0 \\ -k_{s2} & k_{s2} + k_{s3} & \cdot & 0 & 0 & 0 & 0 \\ 0 & \cdot & \cdot & \cdot & 0 & 0 & 0 \\ 0 & 0 & \cdot & \cdot & -k_{sn} & 0 & 0 \\ 0 & 0 & 0 & -k_{sn} & k_{sn} & 0 & 0 \\ 0 & 0 & 0 & 0 & 0 & k_s & 0 \\ 0 & 0 & 0 & 0 & 0 & 0 & k_R \end{bmatrix} \quad (8)$$

$$k_s = \frac{6.77}{(1.79 - \mu)} Grk_R = \frac{2.52}{(1 - \mu)} Gr^3 \quad (9)$$

where G , μ and r are the soil shear modulus, Poisson's ratio and radius for the equivalent circular footing plate, respectively. The damping matrix \mathbf{C} of the total system may then be described depending on damped frame and ground damping parameters in the same form as follows

$$\mathbf{C} = \mathbf{C}_B + \mathbf{C}_S + \mathbf{C}_R + \mathbf{C}_{VD} \quad (10)$$

$$\mathbf{C} = \begin{bmatrix} c_{s1} + c_{s2} + c_{v1} + c_{v2} & -c_{s2} - c_{v2} & 0 & 0 & 0 & 0 & 0 \\ -c_{s2} - c_{v2} & c_{s2} + c_{s3} + c_{v2} + c_{v3} & \cdot & 0 & 0 & 0 & 0 \\ 0 & \cdot & \cdot & \cdot & 0 & 0 & 0 \\ 0 & 0 & \cdot & \cdot & -c_{sn} - c_{vn} & 0 & 0 \\ 0 & 0 & 0 & 0 & c_{sn} + c_{vn} & 0 & 0 \\ 0 & 0 & 0 & 0 & 0 & c_s & 0 \\ 0 & 0 & 0 & 0 & 0 & 0 & c_R \end{bmatrix} \quad (11)$$

$$c_s = \frac{6.21}{(2.54 - \mu)} \rho v_s r^2 c_R = \frac{0.136}{(1.13 - \mu)} \rho v_s r^4 \quad (12)$$

where \mathbf{C} is the total system damping matrix, \mathbf{C}_B is the structural damping matrix of superstructure which includes storey damping coefficients c_{si} , \mathbf{C}_S and \mathbf{C}_R are the ground linear damping matrices including only swaying (c_s) and rocking (c_R) damping coefficients. ρ and v_s are the mass density and the shear wave velocity of soil, respectively. This matrix \mathbf{C} includes the damping coefficients of additional dampers design variables. The added damping matrix \mathbf{C}_{VD} which is optimally obtained, can also be given as

$$\mathbf{C}_{VD} = \begin{bmatrix} c_{v1} + c_{v2} & -c_{v2} & 0 & 0 & 0 & 0 & 0 \\ -c_{v2} & c_{v2} + c_{v3} & \cdot & 0 & 0 & 0 & 0 \\ 0 & \cdot & \cdot & \cdot & 0 & 0 & 0 \\ 0 & 0 & \cdot & \cdot & -c_{vn} & 0 & 0 \\ 0 & 0 & 0 & -c_{vn} & c_{vn} & 0 & 0 \\ 0 & 0 & 0 & 0 & 0 & 0 & 0 \\ 0 & 0 & 0 & 0 & 0 & 0 & 0 \end{bmatrix} \quad (13)$$

Eqs. (1)–(13) for the SSI model were given by Takewaki [50]. It can be decomposed into corresponding damping coefficients of added dampers and is written as

$$\mathbf{C}_{VD} = c_{v1} \frac{\partial \mathbf{C}_{VD}}{\partial c_{v1}} + c_{v2} \frac{\partial \mathbf{C}_{VD}}{\partial c_{v2}} + \dots + c_{vn} \frac{\partial \mathbf{C}_{VD}}{\partial c_{vn}} \quad (14)$$

where c_{vj} ($j = 1, 2, \dots, n$) is the damping coefficient of the j th viscous damper and the partial derivative of \mathbf{C}_{VD} denotes the location matrix of the j th added damper. Considering i th mode, the following equation can be written as

$$2\zeta_i \omega_i = \frac{\phi_i^T \mathbf{C} \phi_i}{\phi_i^T \mathbf{M} \phi_i} = \frac{\phi_i^T (\mathbf{C}_B + \mathbf{C}_S + \mathbf{C}_R) \phi_i}{\phi_i^T \mathbf{M} \phi_i} + \frac{\phi_i^T \mathbf{C}_{VD} \phi_i}{\phi_i^T \mathbf{M} \phi_i} \quad (15)$$

Considering the damped structure, the total damping ratio of the system is defined as ζ_i . The i th mode vector normalized is represented as ϕ_i , and ω_i indicates the natural circular frequency of i th mode of the structural system. There exists no coupling between any other modes and i th mode. The structural damping ratio and added damping ratio of i th mode are symbolized ζ_{si} and ζ_{adi} . It can be conveniently presumed to simplify the formulation of the problem as follows

$$\frac{\phi_i^T (\mathbf{C}_B + \mathbf{C}_S + \mathbf{C}_R) \phi_j}{\phi_i^T \mathbf{M} \phi_j} = \begin{cases} 2\zeta_{si} \omega_i & i = j \\ 0 & i \neq j \end{cases} = \frac{\phi_i^T \mathbf{C}_{VD} \phi_j}{\phi_i^T \mathbf{M} \phi_j} = \begin{cases} 2\zeta_{adi} \omega_i & i = j \\ 0 & i \neq j \end{cases} \quad (16)$$

Equation (15) is rewritten using Eq. (16) as follows:

$$\zeta_i = \zeta_{si} + \zeta_{adi} \quad (17)$$

ζ_{si} is generally given according to the types of structures. ζ_i is the total

damping ratio and ζ_{adi} is called as the added damping ratio for i th mode. It can be calculated as

$$2\zeta_{adi}\omega_i = \frac{\phi_i^T C_{VD}\phi_i}{\phi_i^T M\phi_i} = c_{v1} \frac{\phi_i^T \frac{\partial C_{VD}}{\partial c_{v1}} \phi_i}{\phi_i^T M\phi_i} + c_{v2} \frac{\phi_i^T \frac{\partial C_{VD}}{\partial c_{v2}} \phi_i}{\phi_i^T M\phi_i} + \dots + c_{vn} \frac{\phi_i^T \frac{\partial C_{VD}}{\partial c_{vn}} \phi_i}{\phi_i^T M\phi_i} \tag{18}$$

where a new parameter λ_j can be defined as

$$\lambda_j = \frac{\phi_i^T \frac{\partial C_{VD}}{\partial c_{vj}} \phi_i}{\phi_i^T M\phi_i} \quad (j = 1, 2, \dots, n) \tag{19}$$

To derive the added damping ratio, Eq. (18) can be given by arranging as follows

$$\zeta_{adi} = \frac{1}{2\omega_i} (\lambda_1 c_{v1} + \lambda_2 c_{v2} + \dots + \lambda_n c_{vn}) = \frac{1}{2\omega_i} \sum_{j=1}^n \lambda_j c_{vj} \tag{20}$$

Equations (14)-(20) were derived by Aydin [8] to find optimal damper distribution. Aydin [8] did not consider SSI when modelling the building system while in the present study the effect of ground effect on damping design is investigated by applying the method given by Aydin [8] on the SSI model.

At strong earthquake levels, structural behavior can move to a nonlinear region, which is very important due to its impact on behavior of dampers, and there is still a gap in this regard. This study is based on the assumption of linear behavior for both the structural model and damping behavior. The derived equations, which contain modal behaviors and time history analyses, include a linear response.

3. Damper optimization problem

In the case of structural optimization problems, cost is an important phenomenon. These technological elements, which have been used for the control of the structures in recent years, increase the cost of the building significantly. Since the increase in the capacity of the dampers will lead to an increase in the damping coefficients, the need to minimize the sum of the damping coefficients comes from an economic perspective. The sum of the damping coefficients of dampers is chosen as the proposed objective function to be minimized; it can be given as

$$\text{Min. } f = \sum_{j=1}^n c_{vj} \tag{21}$$

An equality constraint can be considered in terms of added damping ratio as below

$$\zeta_{adi} = \frac{1}{2\omega_i} (\lambda_1 c_{v1} + \lambda_2 c_{v2} + \dots + \lambda_n c_{vn}) \tag{22}$$

ω_i and λ_j ($j = 1, \dots, n$) can be calculated using Eigen analysis. All optimization functions linearly depend on the design parameters. The upper and lower bounds of the design variables, the inequality constraints are given as

$$0 \leq c_{vj} \leq \bar{c} \quad (j = 1, 2, \dots, n) \tag{23}$$

The parameter \bar{c} is defined as the upper limit of each design variable.

In this study, the optimum design of linear viscous dampers is investigated. If there is an exponent of velocity or the damping coefficient, which varies with the damping force, it means that the damper is not linear, and of course, has an impact on the design to be considered for cost minimization. Developing a method on nonlinear dampers will produce much more realistic results for damped structures under strong earthquake effects. In this study, the analyses include linear structures and linear viscous dampers. The equations derived for the damping ratio use modal parameters, therefore the model structure is considered to be linear in the analysis.

There is a changeability in the solution methods of the damper design problem. In the literature, different structural behaviors were chosen either as an objective function or a constraint to find the optimal damper allocation. Some of them were based on active control theory. While the governing equations of some studies were derived in the frequency domain, the others were based on the time domain. While some of the damper design methods use indirect optimization methods, some of them are based on direct optimization methods. Methods that minimize structural behaviors such as displacement, interstorey drifts, acceleration, and forces have been extensively studied in the literature. Although there are highly complicated and advanced methods for damper design, there is a need for easier methods in practical applications. The problem of minimizing costs in building design is considered to be especially important for these devices. The dampers are technological elements and minimizing the amount of damper is cost-effective. The derived equations are simple and straightforward. The total amount of dampers is fixed in many studies and this total amount is distributed according to the structural response. In this study, although there is no limit to the sum of the dampers, an upper bound is taken as a passive constraint for each damper taking into account the production standards of the dampers. The formulations and their solutions on damper optimization must be simple and easy to use as well as the methods covering the structural response. It is thought that the practicality of the proposed method can be associated with the simplicity of the proposed formulation and usability of basic numerical optimization methods. The upper bound on each damping coefficient plays an important role in the proposed optimal damper design. However, in practical applications, a damper capacity and size, which correspond to the upper bound of the added damper, should be restricted because of commercial, manufacturing, and constructional limitations. The damper capacity and location in a storey are generally chosen among available dampers and their locations in practical applications. Therefore, the implication of the upper limit of each damping coefficient can be a useful way of an optimal damper problem.

3.1. Solution algorithm

Some optimization methods have been developed such as gradient-based algorithms [6,48,49], swarm algorithms such as artificial bee and ant colony algorithms [3,44], genetic algorithms and fuzzy logic algorithms [54] in damper optimization. Since the aim and the constraints functions are linear functions of design variables, the problem is easy to solve. To find the optimal values of damping coefficients under constraints by minimizing the objective function, some of the optimization algorithms such as Differential Evolution, Nelder Mead, and Simulated Annealing are used [55]. These three numerical minimization methods have been applied to create an algorithm of optimal damper design [8]. The process steps of the algorithm given in Fig. 2 can be summarized as follows:

- Select a design earthquake record.
- Read the structural mass (M) and stiffness matrices (K). Select the upper limit of the design variable c and the allowable level of interstorey drift ratio IDR .
- Calculate ω_i, ϕ_i , structural damping matrix for i th mode.
- Take iteration number = 1 at the beginning of the algorithm.
- Calculate $\zeta_{adi}^{new} = \zeta_{adi}^{old} + 0.01$ while assume $\zeta_{adi}^{old} = 0$ in the first iteration. ζ_{adi}^{new} is raised by 1% at each iteration.
- Minimize the objective function given in Eq. (21) according to constraints of Eqs. (22)–(23). Use Differential Evolution, Nelder Mead, and Simulated Annealing [55].
- Find a candidate optimum design.
- Test the candidate optimum design found in Step 7 doing time history analysis. In this test, compute $IDR_i = \frac{(\delta_i^{peak}(t) - \delta_{i-1}^{peak}(t))}{h_i}$ for $i = 1, \dots, n$. If all IDR computed are under the allowable level, the

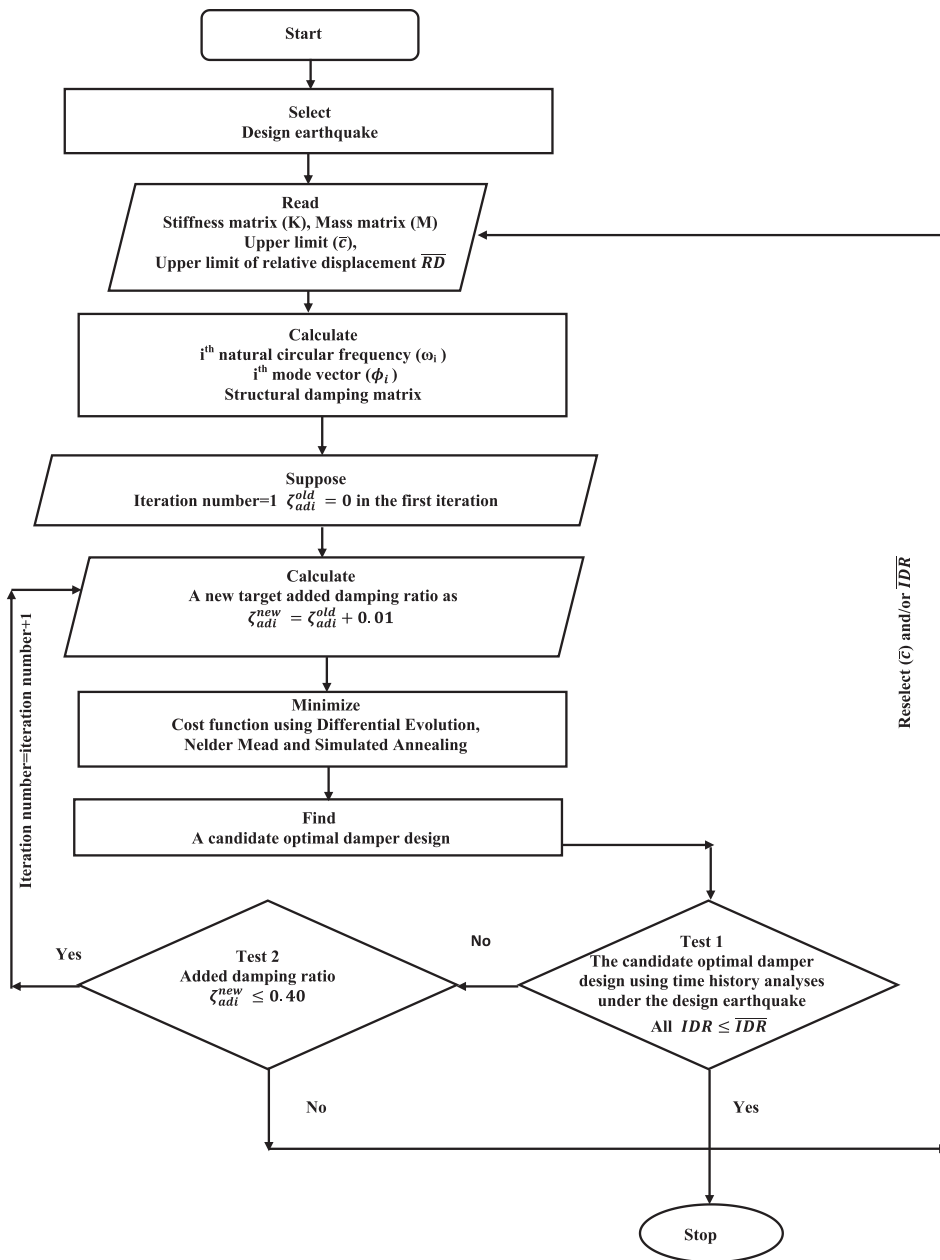


Fig. 2. Flowchart of damper optimization algorithm.

algorithm is finished. Otherwise, return to test 2 as shown in a flowchart.

Control the added damping ratio as $\zeta_{adi}^{new} \leq 0.40$. The maximum damping ratio which can be reached by adding dampers in building type structures is chosen as 0.40. If this step is satisfied, go to step 5 and repeat the iteration by increasing the target damping ratio. If this condition is not satisfied, go to step 2 and reselect \bar{c}_i and/or \bar{IDR} again.

To solve optimization problems, Differential Evolution, Nelder Mead, and Simulated Annealing are commonly used. Differential Evolution is a direct optimization method that is a fast and quite robust stochastic parallel search evolution strategy. Differential Evolution method is a preferred method of solving non-differentiable, non-linear, and multimodal objective functions. One of the popular direct search procedure is Nelder Mead and the algorithm provides a set of points for design variables that form the corners of a polytope n-dimensional space. Simulated Annealing is also a simple stochastic function

minimization that results from the physical annealing process. The procedure inspired from a metal object heating to a high temperature and to cool. The process permits the atomic structure of the metal to settle in a lower energy situation and thus becomes a harder metal [55]. These methods display good consistency between them.

4. Numerical example

The n-storey model seen in Fig. 1 is considered as 5-storey and the proposed method is tested on this model. The masses (m) and mass moment of inertia (I_R) of $m_i = 30 \times 10^3$ kg, $I_{Ri} = 1.6 \times 10^5$ kg m² ($i = 1, \dots, 5$) for each floor, $m_0 = 90 \times 10^3$ kg and $I_{R0} = 4.8 \times 10^5$ kg m² for ground floor are taken respectively [50]. The stiffness coefficient of each floor is taken as 4×10^6 N/m and the damping matrix is calculated in proportion to the mass matrix. The structural damping ratio is selected as 0.02. Every storey height is 3.0 m. The swaying and rocking stiffness coefficients (k_s, k_R) and damping coefficients (c_s, c_R) related to the horizontal motion and

angular motion of the structure-ground interaction are found with the help of Eqs. (9) and (12). The radius of the equivalent circular footing plate is selected as 4 m. Three different soil conditions are considered and the soil properties used in analyses are given in Table 1. The upper limits of the damping coefficient on each floor are selected as 1×10^6 N s/m for first mode control and 0.5×10^6 N s/m for second mode control. It is known that, in practical applications, dampers increase the damping ratio added in building structures up to approximately 40% and the maximum value of added damping ratio is selected in this limit. The allowable level of the IDR used in step 8 of the algorithm is taken as 1%, which is an acceptable value for reducing the risk of damage. El Centro (NS) earthquake acceleration record is used as the design earthquake in the time history analyses.

Using the aforementioned solution algorithm, the optimum damper distribution on the 5-storey construction model is found for four different ground conditions which are rigid, dense sand, medium dense sand, and loose sand. The implementation of this algorithm, developed by Aydın [8], to a 5-storey building model with soil-structure interaction is carried out here. During the numerical analyses described in steps 6 and 7 of the algorithm and minimizing the cost, the variation of the cost function with respect to the design step numbers is shown in Fig. 3 for four soil conditions. In the numerical optimization phase, three different numerical optimizers are used: Nelder Mead, Differential Evolution, and Simulated Annealing. The reason for using three different numerical optimization methods is to verify the results obtained from anyone. The graphs in Fig. 3 refer to the changes during the solutions in the last cycle of the algorithm. For all sandy soil supports and rigid support defined here, it is clear that the cost function converges to a minimum value. The value of the minimum cost function increases as the condition of the structure changes from the rigid to the loose sandy state. The deterioration of the ground condition means an increase in the amount of damper to be used to control that structure. Another result that can be understood from Fig. 3 is that the results obtained for the rigid case, dense sandy, and medium dense sandy soils are close to each other, and otherwise the loose sandy soil condition is different from the others and cost more. In these three cases which give close results, an additional damping ratio of 0.18 is required for the control of the first mode, whereas in the case of loose sand, the additional damping ratio is 0.34.

Similar graphs of numerical optimization histories can be drawn for the control of the second mode as shown in Fig. 4. Furthermore, besides controlling the first mode, control of the second mode is also performed separately. Descriptions similar to the first mode may be made within the control of the second mode in terms of the value of the objective (cost) function. In the second mode, the looseness in the sandy soil increases the amount of damper added.

Fig. 5 shows how the damper coefficients are distributed to the floors of the building in first and second mode control. While the rigid support, dense sandy soil and medium dense sandy soil cases also give the damper distributions close to each other, the optimum damper distribution in the loose sandy soil condition is different from the other. Total damper coefficients are found as 1,272,094 Ns/m (rigid), 1,275,869 Ns/m (dense sand), 1,287,405 Ns/m (medium dense sand) and 3,047,626 Ns/m (loose sand). In the case of loose sand, the dampers are distributed to the first four floors while in other cases they are distributed in the first two floors for first mode control. In Fig. 3, it can

be said that the less amount of damper is needed in case of control of the second mode. The upper limit of the damping coefficient is reduced by half in order to see the damper distribution for different soil conditions more clearly in second mode control. In terms of the total damper cost, it is seen that the loosely sanded condition is slightly different from the others. In the first mode, the dampers follow a trend in decreasing amounts to upper floors from the lower floors, while the dampers are distributed to the 1st, 4th and very few 5th floors in the second mode control. Damper locations vary depending on the mode behaviour controlled. It is observed that rigid, dense, and medium dense sandy soil conditions have similar results, while loose sandy soil condition produces different distributions than the others. The looseness of the sandy soil means more damping coefficient and damper to be placed on more floors. The stiffness and damping parameters of the soil in Eqs. (9) and (12) change with the variation in the denseness of sandy soil given in Table 1. The stiffness and damping coefficients decrease from the dense sandy soil to the loose sandy soil. With the decrease of these values, displacements increase in the building model. Moreover, there are changes in the modal behavior of the SSI model. These changes, which occur with the difference in sandy ground, also affect the optimal damper distribution.

The aforementioned algorithm includes time history analyses under a design earthquake in each cycle. In each cycle, the optimal damped structural model with earthquake loads is checked whether all IDRs fall below the allowable level. The IDR specified here is the peak IDR values obtained from time history analyses. If all IDRs do not fall below the desired level, the operation of the algorithm is continued by increasing the added target damping ratio. If all IDRs fall below the allowable level, the algorithm is stopped and the target damping ratio is reached in that step. Fig. 6 shows the variation of the IDRs in each cycle with the added damping ratio for different soil conditions. As can be seen from this figure, for the case of rigid supports and three different soil conditions, all of the IDRs at the end of the algorithm are reduced below the allowable level (1%). While the $IDR-\zeta_{ad1}$ change is very close to each other in the rigid support, dense and medium dense sand soil conditions, the change of loose sandy soil is different from the others. In the case of rigid, dense sand and medium dense sand, the algorithm is going up to step 18, whereas in the loosely sandy soil state the loop ended in step 34 for the first mode control. In the second mode, Fig. 7 shows that all IDRs are reduced below the allowable level. Only in the case of the loose sandy soil, the added damping ratio of the second mode reaches 40%, while it reaches 38% in the other cases.

The profiles of the IDRs of the structures with and without optimal dampers are plotted in Fig. 8 in the case of first and second mode control. When the first mode control is examined, the IDR is lowered below the allowable level in all cases with dampers. Furthermore, when the IDRs on the floors are examined, it can be stated that the best performance of the damper designs is generally provided by the loose sandy soil condition except for the 4th floor. In the case of the control of the second mode, when the second graphic of Fig. 8 is examined, the performance of all soil states is seen to be very close to each other except for IDR of the 4th floor in the loose sandy soil. Analyses have shown that the weakness in structural behaviour resulting from sandy soil can be eliminated by the optimal use of dampers, closer to the behaviour of the rigid condition, and even better.

A comparison is needed to verify the method and the model shown. Although it is difficult to find a similar approach in the literature, there are some methods of optimal damper design. One of the most well-known among these is the method developed by Takewaki [48] where the optimal damper distribution is calculated using the transfer functions, and the “Steepest Direction Search Algorithm” (SDSA) is shown. In that study, the optimum damper distribution on a planar frame is realized by considering the first mode effect. The effects of soil-structure interaction are not taken into consideration and the supports are defined rigidly. By applying this method to the SSI model in this study, the optimum damping distribution with the transfer functions is used to

Table 1
Soil properties used in analyses [11,14].

Soil type	v_s (m/s)	ν	G (MPa)		ρ (kg/m ³)
			Static	Dynamic	
Loose sand	150	0.25	8	33	1450
Medium dense sand	300	0.30	15	151	1650
Dense sand	550	0.35	24	570	1850

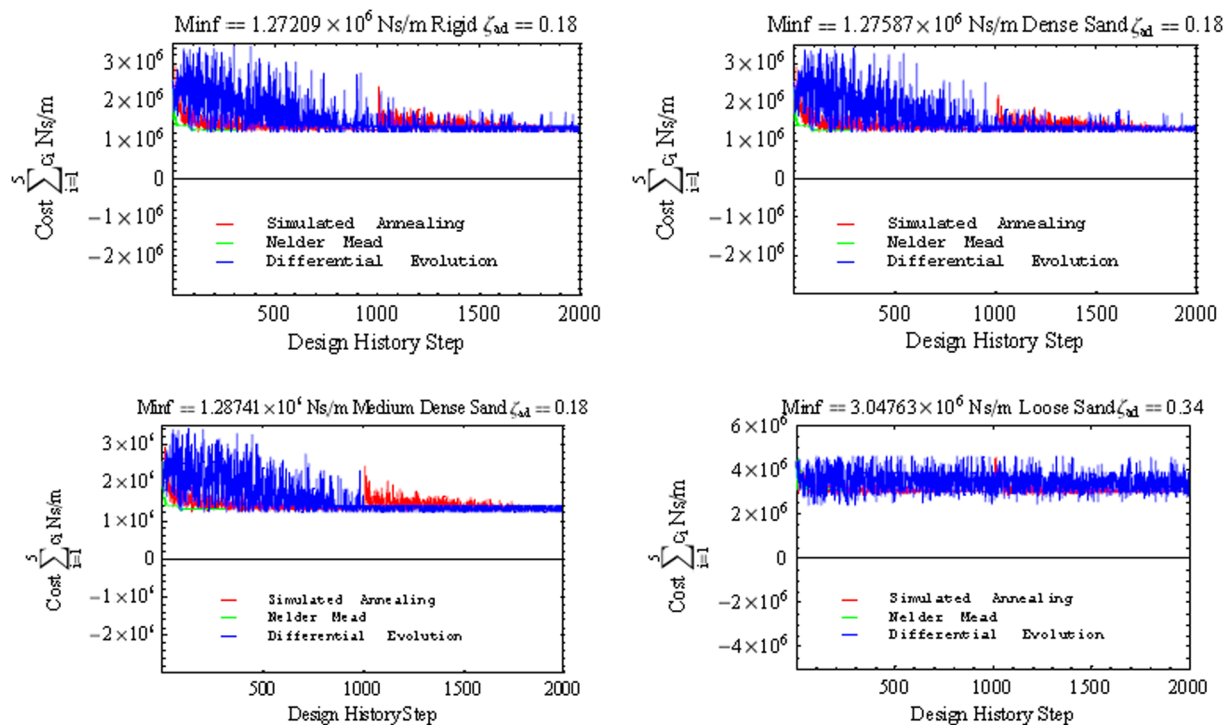


Fig. 3. Variation of cost function according to design history step in case of different soil conditions for first mode control.

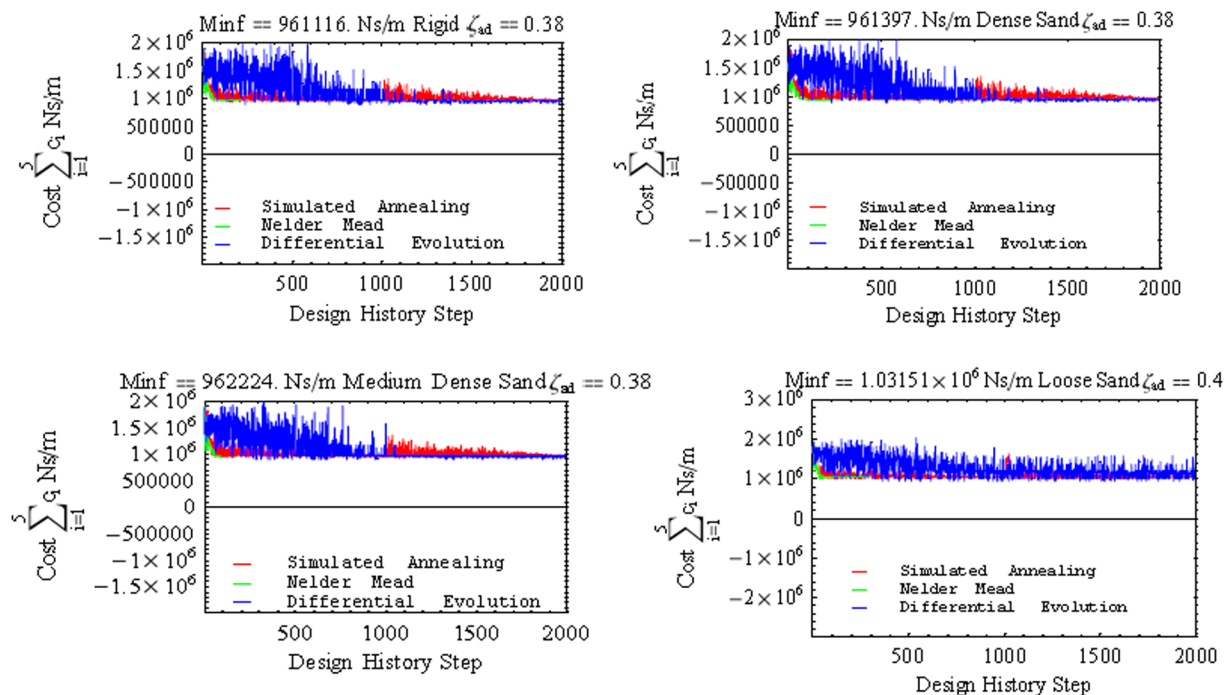


Fig. 4. Variation of cost function according to design history step in case of different soil conditions for first mode control.

make a comparison with the proposed method here. Takewaki's method is based on the principle of minimizing the sum of the interstorey drifts expressed in connection with the transfer functions taking into account the fundamental mode response of the structure. The nonlinear equations that occur by minimizing the function defined using the Lagrange multipliers method are solved with the "Steepest Direction Search Algorithm" (SDSA) and optimum damping coefficients are found. As a constraint of optimization, the total damper coefficient and the upper/lower limits are included in the problem as an equality constraint and inequality constraints. There is not any constraint for the total damper

coefficient in the proposed method in this study. In order to compare the proposed method with Takewaki's method, the sum of the damping coefficients of dampers found by the method shown here is used in Takewaki's method as an active constraint, optimum values are calculated and a comparison is made. The fundamental frequency of the building model has been used in solutions with transfer functions, and the second mode behavior has not been studied. In order to compare the designs found according to the second mode in this study, Takewaki's [48] method is also adapted to find optimal damper design according to the second mode behaviour on the SSI model.

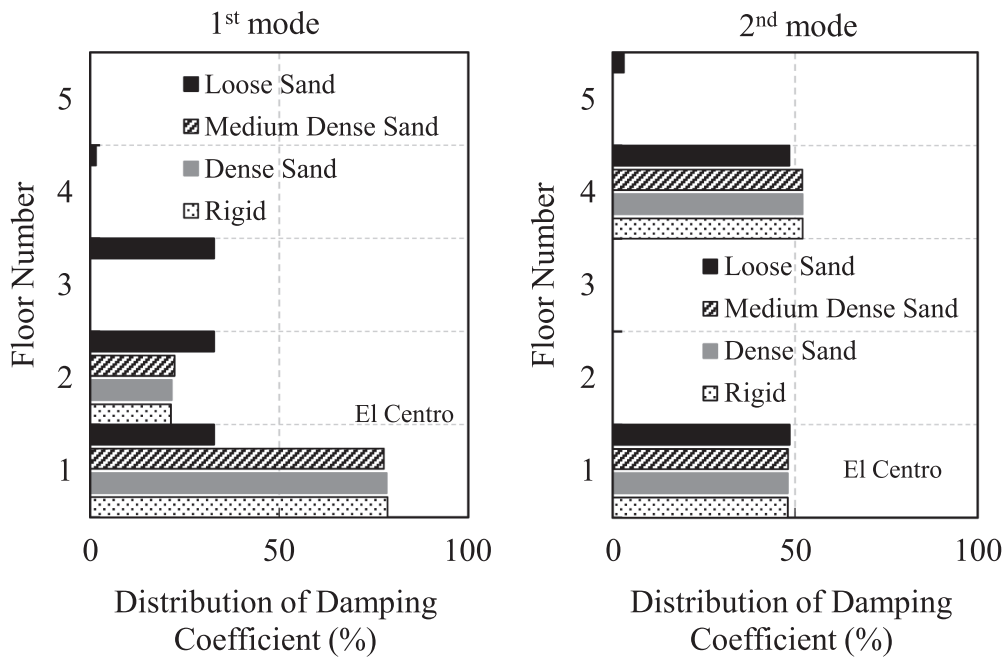


Fig. 5. Optimal damper distributions correspond to different soils conditions in case of first and second mode control.

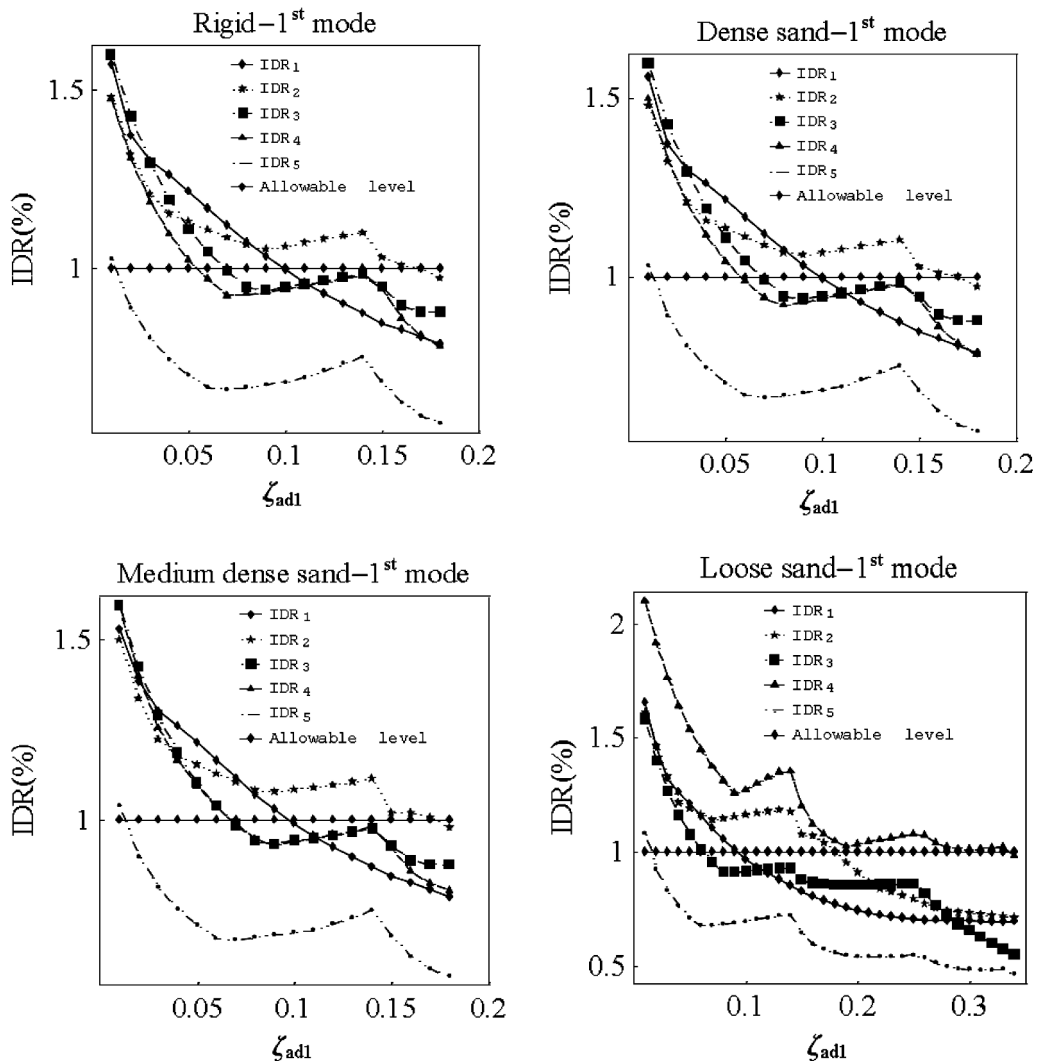


Fig. 6. The variation of IDR according to added damping ratio at the first mode for different soil condition.

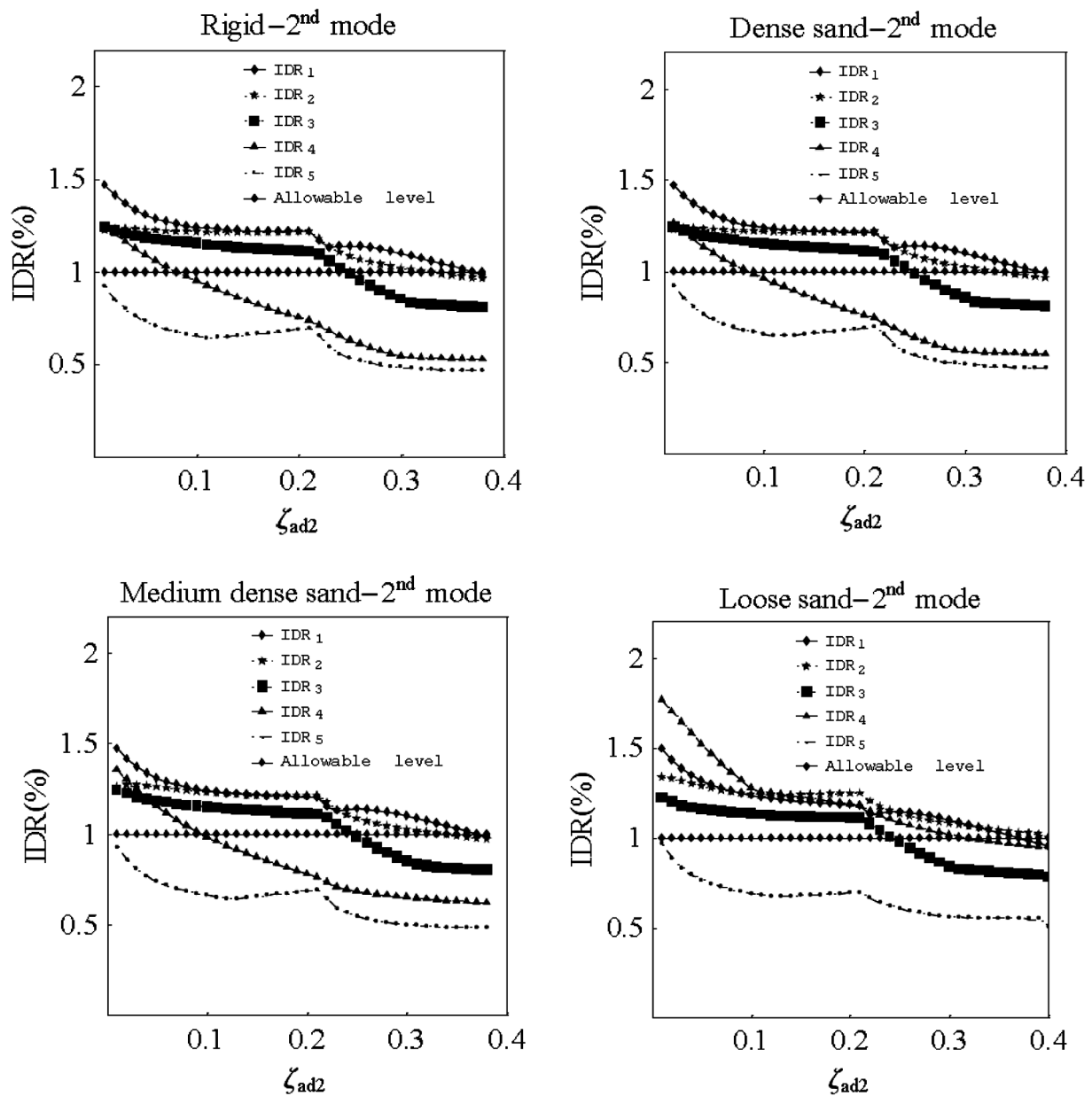


Fig. 7. The variation of IDR according to added damping ratio at the second mode for different soil condition.

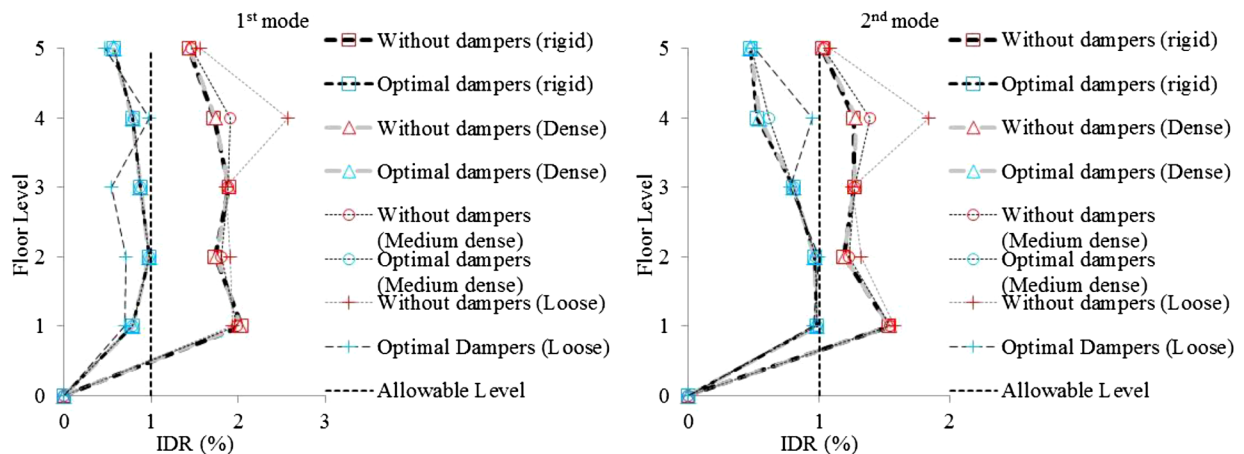


Fig. 8. Peak IDR profiles with and without damper for different soil conditions.

Table 2
Comparison of optimal damper designs.

Soil Type	Modal Response	Optimal Design for the Proposed Method		Optimal Design for Transfer Functions [48]		
		1st Mode	2nd Mode	1st Mode	2nd Mode	
Rigid	c ₁ (%)	78.61	47.98	56.33	9.33	
	c ₂ (%)	21.39	–	43.67	–	
	c ₃ (%)	–	–	–	26.00	
	c ₄ (%)	–	52.02	–	30.33	
	c ₅ (%)	–	–	–	34.34	
	W (Ns/m)	1,272,094	961,116	1,272,094	961,116	
Dense Sand	ζ _{ad}	0.18	0.38	0.173552	0.270963	
	c ₁ (%)	78.38	48.00	56.33	9.67	
	c ₂ (%)	21.62	–	43.67	–	
	c ₃ (%)	–	–	–	26.00	
	c ₄ (%)	–	52.00	–	30.33	
	c ₅ (%)	–	–	–	34.00	
Medium Sand	W(Ns/m)	1,275,869	961,397	1,275,869	961,397	
	ζ _{ad}	0.18	0.38	0.173617	0.272001	
	c ₁ (%)	77.68	48.04	56.33	9.67	
	c ₂ (%)	22.32	–	43.67	–	
	c ₃ (%)	–	–	–	25.67	
	c ₄ (%)	–	51.96	–	30.33	
Dense Sand	c ₅ (%)	–	–	–	34.33	
	W (Ns/m)	1,287,405	962,224	1,287,405	962,224	
	ζ _{ad}	0.18	0.38	0.173815	0.271227	
	Loose Sand	c ₁ (%)	32.81	48.47	32.81	10.00
		c ₂ (%)	32.81	–	32.81	–
		c ₃ (%)	32.81	–	32.81	25.33
c ₄ (%)		1.57	48.47	1.57	30.00	
c ₅ (%)		–	3.06	–	34.67	
W (Ns/m)		3,047,626	1,031,507	3,047,626	1,031,507	
Loose Sand	ζ _{ad}	0.34	0.40	0.340007	0.287722	

The above-mentioned sample problem is solved with transfer functions and optimum designs are obtained. The optimum damping coefficients based on the transfer function method and the results of the proposed method are shown in Table 2 as a percentage. When the results of the four different soil conditions are examined for the first two modes of the building model, the optimal parameters of the two different methods, especially calculated according to the first mode, are quite compatible. The differences are noticeable in the results found according to the second mode. These two different methods have different purposes. While Takewaki's method minimizes the amplitude of the sum of the interstorey drifts, the aim of this study is to achieve a target interstorey drift ratio and a modal damping ratio under the effect of an earthquake. Especially considering the effectiveness of the first mode in the structures, it is seen that the results of the two methods are compatible. The results in Table 2 indicate that changing the sandy soil from rigid to loose causes dampers to be placed on more floors. While it can be seen that rigid, dense and medium-dense sandy soils produce similar optimal designs, the results of the loose sandy soil are quite different from the others, and the results of both methods support this for designs according to the first mode. While the dampers are generally placed on the first and fourth floors in the proposed method in case of the second mode, they are distributed to other floors except the second floor in the other method. When the damping ratios according to the second mode are examined, it can be seen that the proposed method produces higher damping ratios, which also satisfies the interstorey drift ratios below a target value under the design earthquake.

When Table 2 is examined, the optimum designs found by two different methods according to the first mode are compatible with all different ground conditions in terms of damper locations. There are small differences in damping coefficients between the two methods. This compatibility can also be seen, when the damping ratios after the optimum dampers are added to the structure in the first mode. Both

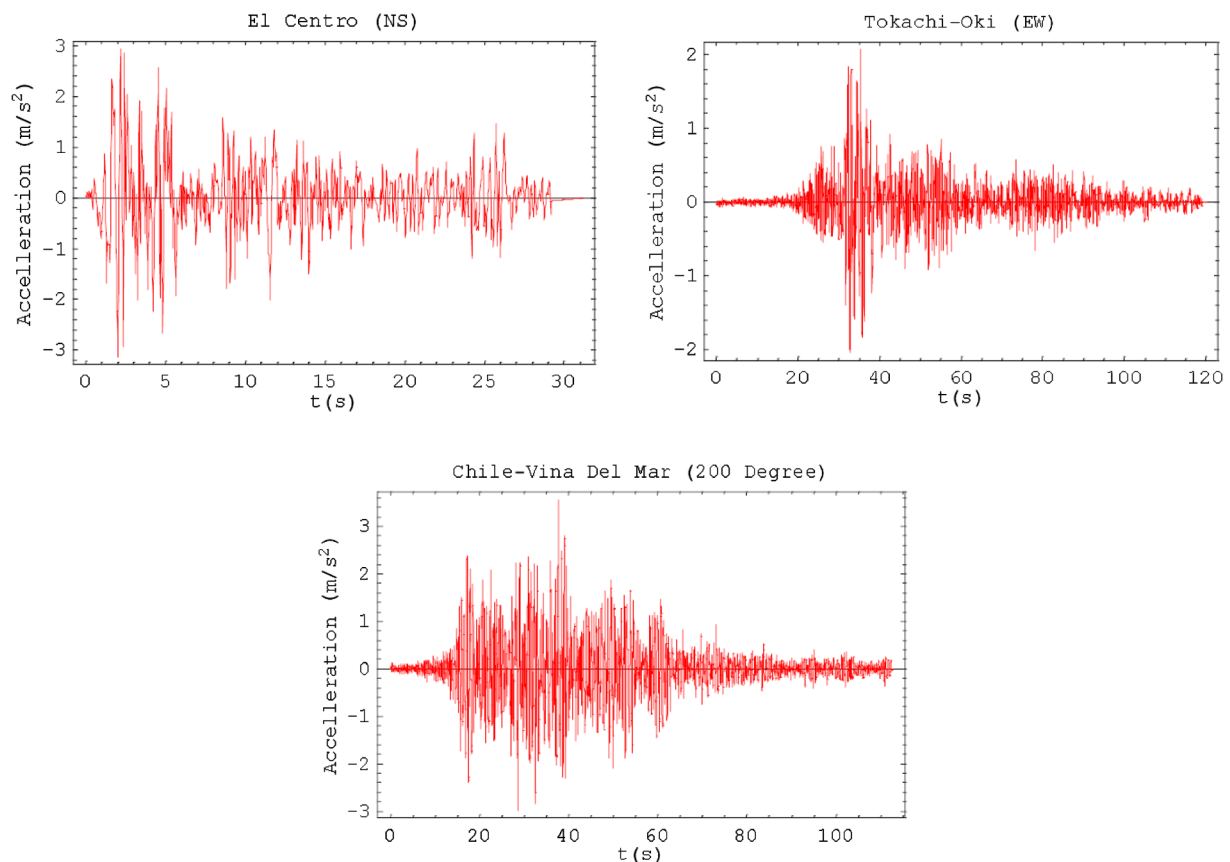


Fig. 9. Design earthquake records.

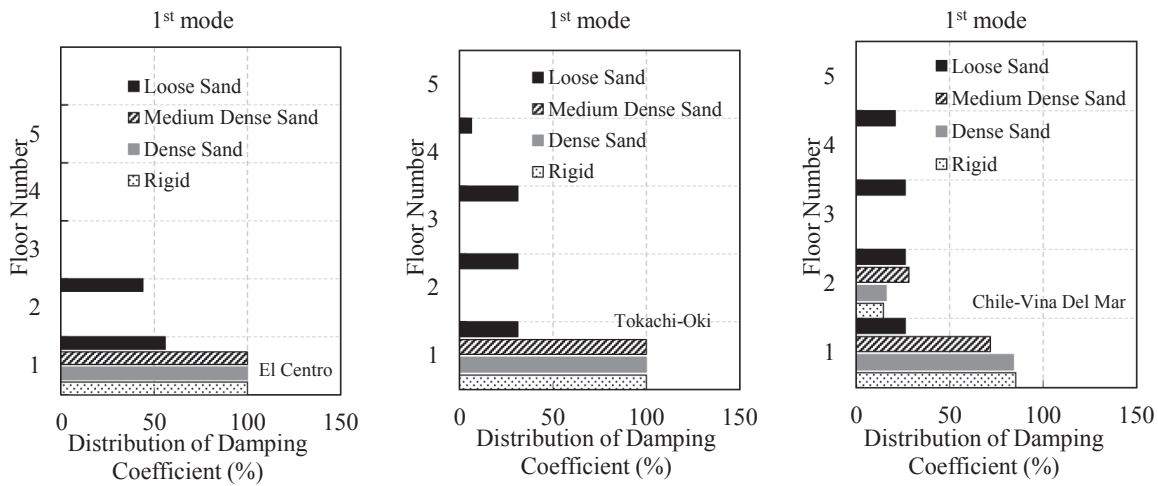


Fig. 10. Optimal damper distributions according to the first mode for different design earthquake records.

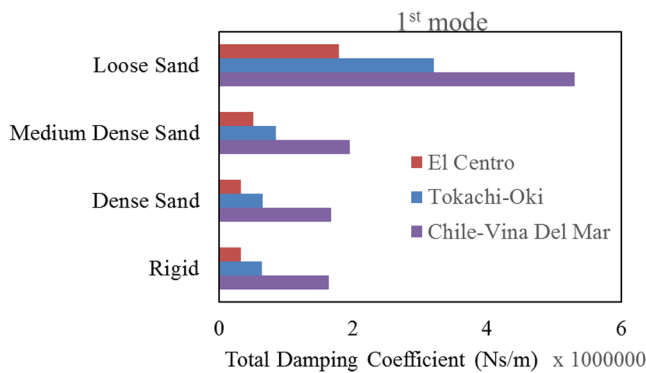


Fig. 11. Variation of the total damping coefficient for both different design earthquake and four ground conditions in case of the first mode.

methods can be used in the solution of the optimum damper problem according to the first mode for different ground conditions. However, it is seen that the large discrepancies occur in the designs according to the second mode. The related work of Takewaki [48] focused on the first mode, while the second or other modes are not considered. The objective function and the other governing equations are defined depending on the absolute values of the transfer functions. In order to make a comparison in the second mode, his method is modified according to the second natural frequency of the structure here. More detailed studies are required on damper designs according to the second mode based on the transfer function. Takewaki's method, which is based on the transfer functions, deals with the optimum distribution of an available total damper coefficient when using the response function calculated according to the first mode. The optimal design based on

transfer functions should be tested under earthquake effect later. While the optimum damper design is found here in the proposed study, a target damping ratio and IDR under a design earthquake are taken into account. Therefore, its behavior under earthquake effect is included in the problem during optimum damper design.

In order to understand the effect of different earthquakes on the optimum damper distribution, only the storey stiffness of the building model given above is changed to 2.2×10^7 N/m, and the optimum dampers are investigated for three different earthquakes given as El Centro, Tokachi-Oki and Chile as shown in Fig. 9. The proposed method uses the linear time history analyses to test whether a target response is reached. For the damping ratio added to the structure, 40% is an acceptable ratio that can be approximately achieved with dampers. This upper limit value is used for the damping ratio added in this study. When using ground motions with high earthquake accelerations, the IDR behavior of the structure cannot be reduced to the desired levels with the addition of only viscous dampers. After the damping ratio reaches 40%, viscous dampers cannot be added further. Therefore, in these cases, IDR values should be decreased by increasing the stiffness of the structure.

While the optimum damper distributions on the new building model under these three different earthquakes are found for both the first mode and second mode behaviors, the ground is modeled as rigid, dense sandy, medium dense sandy, and loose sandy. While the upper limit of each damper in the optimization stage is selected as 1×10^6 Ns/m in the case of El Centro and Tokachi-Oki earthquakes for the first mode control, it is selected as 1.4×10^6 Ns/m in case of Chile earthquake. In cases where the upper limit is insufficient, the designer can consider changing this value, which is a setting parameter, considering the production standards. If the optimum design cannot be achieved, optimization can be achieved by changing the upper limit

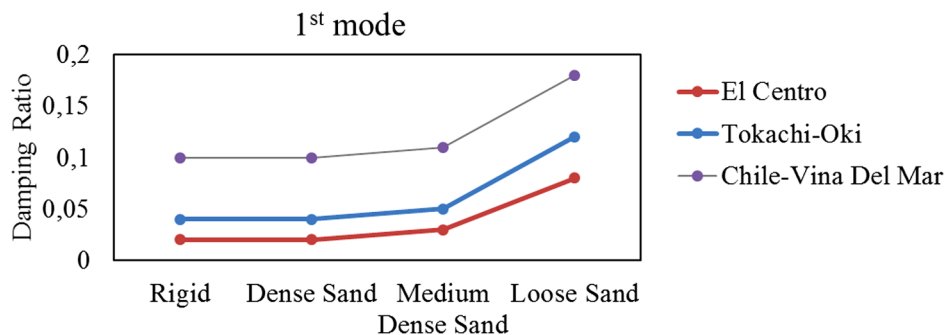


Fig. 12. Added damping ratio for three design earthquake records in case of the first mode control.

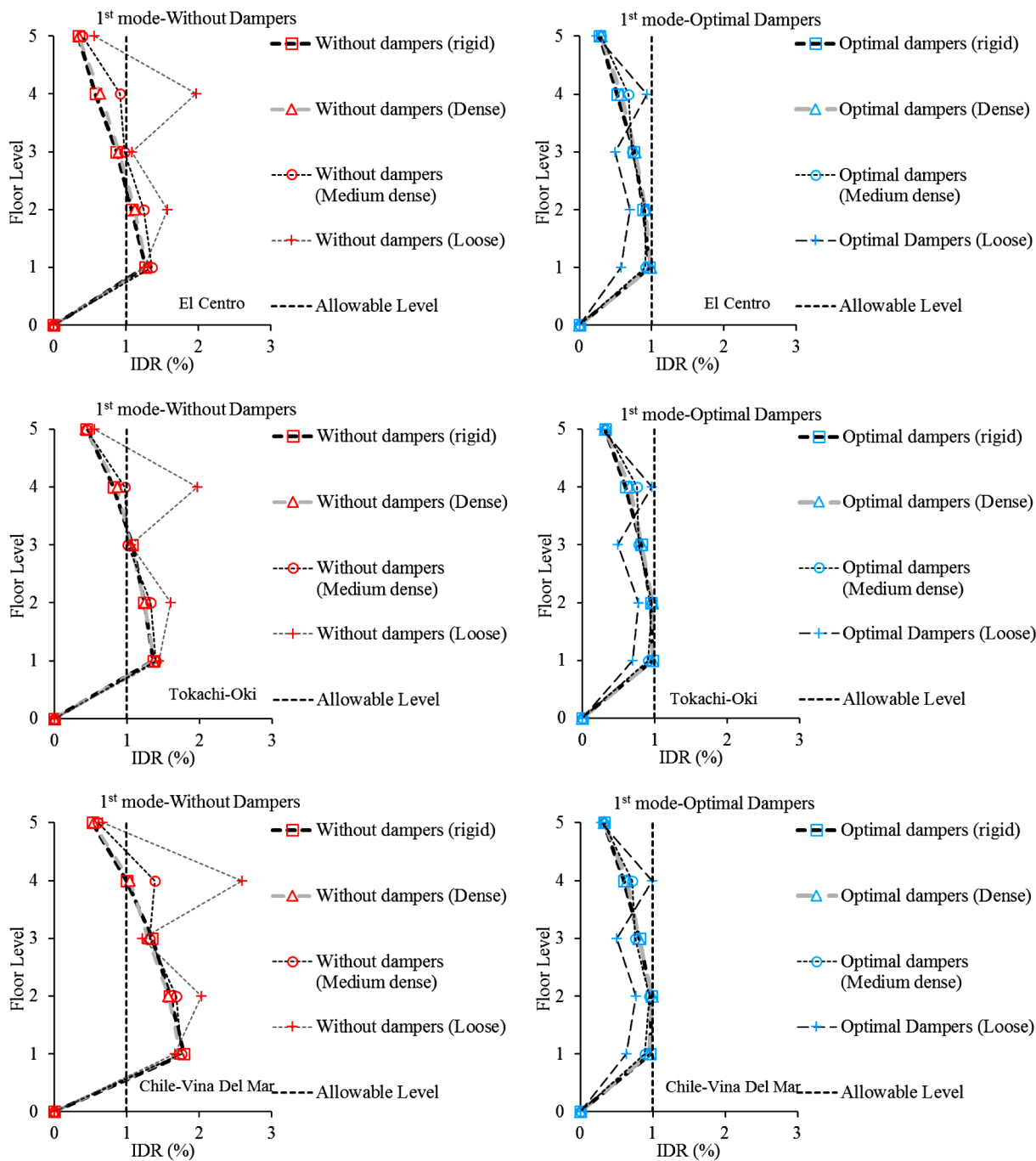


Fig. 13. Peak IDR profiles with and without damper for both different soil conditions and different design earthquakes in first mode.

parameter of the damper accordingly. In this example, since the upper limit value of 1×10^6 Ns/m selected in the first two earthquakes is not sufficient under the Chile earthquake, it is increased to 1.4×10^6 Ns/m and the optimum design is achieved.

Optimal damper distributions according to the first mode can be seen in Fig. 10. While the optimal distributions of rigid, dense sand and medium sand ground conditions are close to each other, the designs that correspond to the loose ground condition are different under all three earthquake records. When analyzed in terms of dampers placed on the floors, dampers are placed on fewer floors under the El Centro earthquake record, while they are distributed to more floors under the Chile earthquake record. This situation becomes more evident especially in the case of loose sandy soil. Among the designs according to these three earthquakes, the design under the Tokachi-Oki earthquake

record can be considered as the second in terms of the distribution of dampers to the floors. When three different designs are examined in terms of the total damper coefficient considering cost, as can be seen in Fig. 11, while the lowest cost is seen in the design for the El Centro, the biggest cost is for the Chile earthquake. Changing the ground from rigid to loose is another important situation that significantly increases the cost. Moreover, the deterioration of the ground reveals that there is a need for a more damping ratio as shown in Fig. 12. This situation is valid for all three earthquakes. In particular, the peak accelerations of Chile and El Centro earthquake records are closer to each other, while that of the Tokachi-Oki earthquake is lower. The differences in the frequency content of these earthquake records can cause different effects on the modal behavior of the building model. As a result, different damper designs may emerge for different earthquakes.

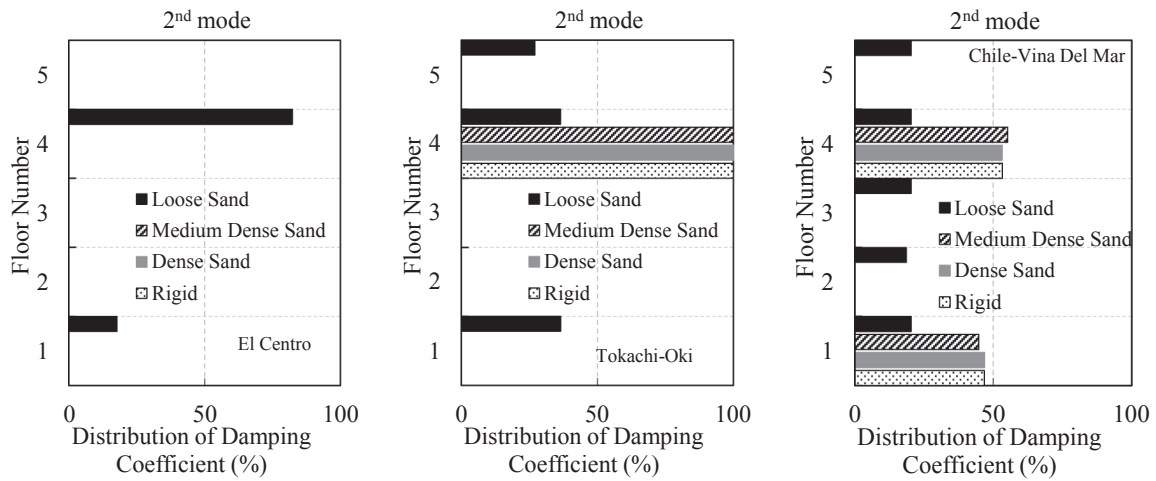


Fig. 14. Optimal damper distributions according to the second mode for different design earthquake records.

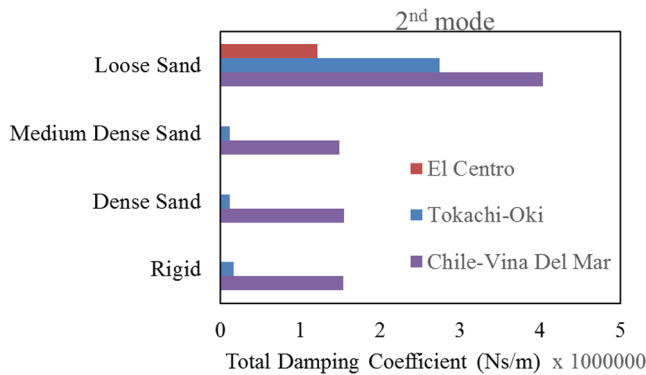


Fig. 15. Variation of the total damping coefficient for both different design earthquake and four ground conditions in case of the second mode.

For all design earthquakes, it is clearly seen that some IDRs exceed the allowable limit as shown in Fig. 13, and these values are reduced below the allowable limit after the optimum damper is placed. Optimal designs found considering the first mode behavior perform quite well in terms of lowering the IDRs below the allowable level. The proposed method controls the values on all floors taking into account the IDRs in terms of structural behavior and investigates new optimum designs until they reach the desired performance. The designer can use other structural performance parameters in this testing phase of the algorithm. The method is also available to adapt to new behavior parameters.

While the upper limit of each damper is selected as 1×10^6 Ns/m in the case of El Centro and Tokachi-Oki earthquakes for the 2nd mode control, it is selected as 0.82×10^6 Ns/m in case of Chile earthquake. As

can be observed from Fig. 14, dampers generally focus on the 1st and 4th floors in case of the second mode control. This is because the placement of the optimum designs are related to the second mode behavior of the structure. When the optimum designs for the El Centro earthquake are examined, it is observed that it is not necessary to add any damper in the case of rigid, dense sand and medium dense sand. Since the calculated IDR values are below the allowable level, the algorithm reaches the target at the initial stage. Optimum designs are found in the case of loose sand and the damper placement on the 1st and 4th floors emerges for the El Centro earthquake. In Tokachi-Oki earthquake, a small number of dampers are placed on the 4th floor in the case of rigid, dense sand and medium dense sand, while in the case of loose sandy ground, dampers are distributed to the 1st, 4th and 5th floors. Compared to the El Centro earthquake, the damper is placed on more floors and costs more in Tokachi-Oki earthquake. When the three design earthquakes are compared, it can be seen that the maximum amount of damper and the highest distribution to different storeys occur in optimum damper design according to the Chile earthquake.

In the case of controlling the second mode, the total damping coefficient amounts are calculated both for different earthquakes and for different ground conditions which are shown in Fig. 15. In Fig. 16, the changes of the damping ratio calculated after the addition of optimal dampers to the structure are plotted both for different design earthquakes and different ground conditions. As can be understood from the analyses, different design earthquakes reveal different damper designs. Moreover, the deterioration of the ground brings the need for extra damping and a higher damping ratio.

The positive effect of optimum designs found on the IDRs of the building model considering the second mode behavior can be seen in Fig. 17. In these graphs, where damper and without damper conditions are compared, it is observed that optimum designs reduce all IDRs

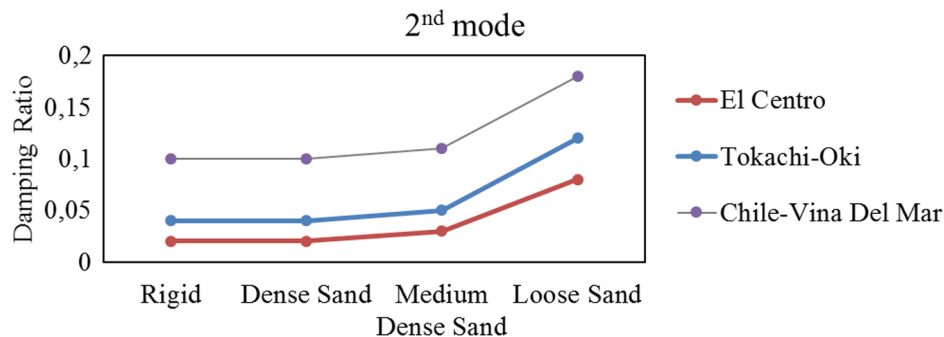


Fig. 16. Added damping ratio for three design earthquake records in case of the second mode control.

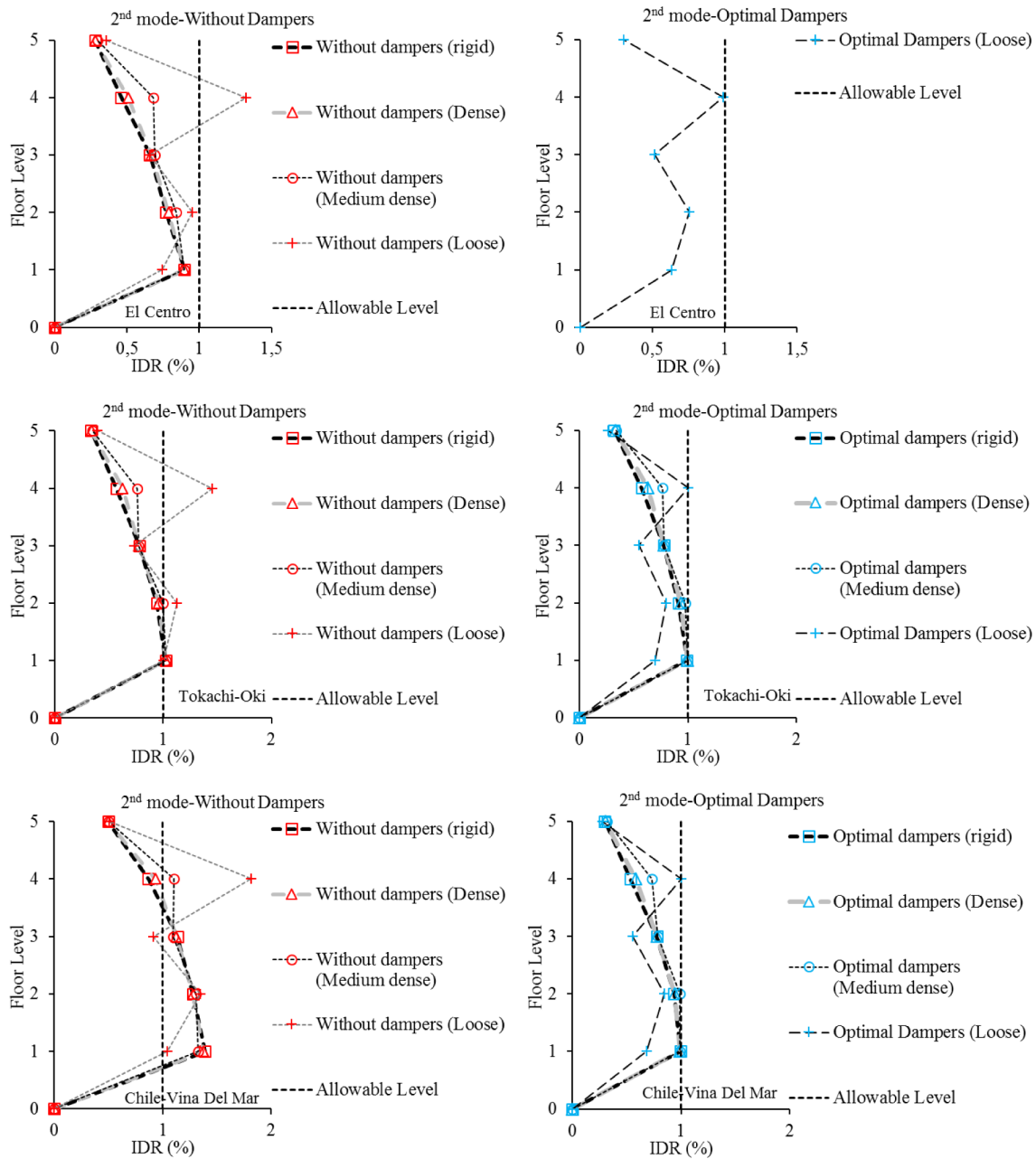


Fig. 17. Peak IDR profiles with and without damper for both different soil conditions and different design earthquakes in the second mode.

below the allowable levels in all different earthquakes and different ground conditions. In the case of El Centro with damper, only the graph in the form of a loose sandy ground is drawn, since no damper is required to be added when the IDRs are initially below the permissible level in the case of rigid, dense sand and medium dense sand.

5. Conclusions

The optimization of dampers has been a focus of earthquake engineering and structural dynamics communities in recent years. In many studies, the ground is taken as rigid. The modelling of soil and structure together in this problem can lead us to more realistic solutions. Moreover, the disadvantages due to ground and structural behaviour can be eliminated by dampers. For this purpose, in this study, damper optimization is investigated in different sandy soil conditions and in rigid support conditions. The damping optimization method developed by Aydın [8] is a method based on a target damping ratio

and a target IDR. Within the scope of this study, the method is applied to a model that takes into account the SSI. The damper distribution which controls the second mode of the structure has also been investigated for different sandy ground and rigid conditions.

The results can be summarized as follows:

- This study has proven that the soil condition plays an important role in the optimal damper problem based on the added damping ratio and target interstorey drift ratio (IDR).
- The relative density of sandy soil has an effect on the optimal damper distributions found by minimizing the cost function. Especially, in the case of loose sandy soil, different results for the first mode control are obtained depending on the conditions of dense sandy, medium dense sandy, and rigid support. All designs with the result of control of the second mode are closer to each other according to the first mode.
- As the looseness of the sandy soil increases, the cost function and the

number of the damper locations increase especially in the control of the first mode. This increase is less in control of the second mode.

- The amount of damper (cost) required to control the first mode with damper optimization is greater than that required for control of the second mode for all sandy soil conditions mentioned in this paper.
- Different design earthquakes can reveal different damper designs. Moreover, the deterioration of the ground brings the need for extra damping and higher damping ratios.
- By applying a method adapted for sandy soils, the disadvantages of the sandy soil can only be resolved by using optimum dampers without any improvement in the ground.

Declaration of Competing Interest

The authors declare that they have no known competing financial interests or personal relationships that could have appeared to influence the work reported in this paper.

Author contributions

E-A and B-O contributed to the conception and idea of the paper. The analyses of the optimization were carried out in Mathematica 5.0 by E-A and B-O. The introduction section and literature review were prepared by A-B and EN-F. A-B and EN-F contributed to organize, read, review, and approve the submitted version.

Contribution to the field statement

The optimization of viscous dampers has been remarkable in the field of structural engineering and earthquake engineering in recent years. Many methods in the literature have been developed to find the optimum damper distribution. In this study, the optimum design of viscous dampers was found based on the target damping ratio and relative displacement ratio, which is one of the methods in the literature. The soil-structure interaction model was established and the optimum design of the dampers for different sandy soils was investigated. The results of the study show that the optimum damper distribution and the behaviour of the structure change as the stiffness of the sandy ground decreases. Furthermore, the negative structural behaviours caused by sandy soil can be improved by optimal dampers.

References

- [1] Akehashi H, Takewaki I. Comparative investigation on optimal viscous damper placement for elastic-plastic MDOF structures: transfer function amplitude or double impulse. *Soil Dyn Earthq Eng* 2020;130:105987.
- [2] ASCE/SEI 7. Minimum design loads and associated criteria for buildings and other structures. American Society of Civil Engineers, Reston, VA; 2016.
- [3] Amini F, Ghaderi P. Hybridization of harmony search and ant colony optimization for optimal locating of structural dampers. *Appl Soft Comput* 2013;13:2272–80. <https://doi.org/10.1016/j.asoc.2013.02.001>.
- [4] Arboleda-Monsalve LG, Mercado JA, Terzic V, Mackie KR. Soil-structure interaction effects on seismic performance and earthquake-induced losses in tall buildings. *J Geotech Geoenviron Eng* 2020;146(5):04020028.
- [5] Ashour SA, Hanson RD. Elastic response of buildings with supplemental damping. Technical Report UMCE 1987:87–91.
- [6] Aydın E, Boduroglu MH, Guney D. Optimal damper distribution for seismic rehabilitation of planar building structures. *Eng Struct* 2007;29:176–85. <https://doi.org/10.1016/j.engstruct.2006.04.016>.
- [7] Aydın E. Optimal damper placement based on base moment in steel building frames. *J Constr Steel Res* 2012;79:216–25.
- [8] Aydın E. A simple damper optimization algorithm for both target added damping ratio and interstorey drift ratio. *Earthq Struct* 5 (1); (2013): 083–109. <https://doi.org/10.12989/eas.2013.5.1.083>.
- [9] Aydın E, Ozturk B, Dutkiewicz M. Analysis of efficiency of passive dampers in multistorey buildings. *J Sound Vib* 2019;439:17–28. <https://doi.org/10.1016/j.jsv.2018.09.03>.
- [10] Bektaş G, Nigdeli SM. Metaheuristic based optimization of tuned mass dampers under earthquake excitation by considering soil-structure interaction. *Soil Dyn Earthq Eng* 2017;92:443–61. <https://doi.org/10.1016/j.soildyn.2016.10.019>.
- [11] Bowles JE. Foundation analysis and design. 5th ed. New York: The McGraw-Hill Companies Inc; 1996.
- [12] Bogdanovic A, Rakicevic Z, Noroozinejad Farsangi E. Shake table tests and numerical investigation of a resilient damping device for seismic response control of building structures. *Struct Control Health Monit* 2019;26(11):e2443.
- [13] Cao X, Mlejnek HP. Computational prediction and redesign for viscoelastically damped structures. *Comput Methods Appl Mech Eng* 1995;125(1–4):1–16. [https://doi.org/10.1016/0045-7825\(95\)00798-6](https://doi.org/10.1016/0045-7825(95)00798-6).
- [14] Carter M, Bentley SP. Soil properties and their correlations. 2nd ed. Wiley; 2016. ISBN: 978-1-119-13087-1.
- [15] Cetin H, Aydın E, Ozturk B. Optimal damper allocation in shear buildings with tuned mass dampers and viscous dampers. *Int J Earthq Impact Eng* 2017;2(2):89–120.
- [16] Cetin H, Aydın E, Ozturk B. Optimal design and distribution of viscous dampers for shear building structures under seismic excitations. *Front Built Environ* 2019. ID: 454069.
- [17] Chameski S. Structural rigidity in calculating settlements. *J Soil Mech Found Divis* 82(1); 1956: 1–19. <https://cedb.asce.org/CEDBsearch/record.jsp?dockey=0010800>.
- [18] Constantinou MC, Tadjbakhsh IG. Optimum design of a first storey damping. *Comput Struct* 1983;17(2):305–10. [https://doi.org/10.1016/0045-7949\(83\)90019-6](https://doi.org/10.1016/0045-7949(83)90019-6).
- [19] El Ganainy HM, El Naggar MH. Efficient 3D nonlinear Winkler model for shallow foundations. *Soil Dyn Earthq Eng* 2009;29(8):1236–48. <https://doi.org/10.1016/j.soildyn.2009.02.002>.
- [20] EuroCode 8. Design of structures for earthquake resistance. Part 5: foundations, retaining structures and geotechnical aspects; 2004.
- [21] Farsangi EN, Tasnimi AA, Yang TY, Takewaki I, Mohammadhasani M. Seismic performance of a resilient low-damage base isolation system under combined vertical and horizontal excitations. *Smart Struct Syst* 2018;22(4):383–97.
- [22] Gürğöze M, Müller PC. Optimum position of dampers in multi body systems. *J Sound Vib* 1992;158(3):517–30. [https://doi.org/10.1016/0022-460X\(92\)90422-T](https://doi.org/10.1016/0022-460X(92)90422-T).
- [23] Guzman T. Heavily loaded strap footing-design, detailing and behaviour. *Struct Mag* 2010;2010:12–5.
- [24] Hahn GD, Sathivageeswara KR. Effects of added-damper distribution on the seismic response of building. *Comput Struct* 1992;43(5):941–50. [https://doi.org/10.1016/0045-7949\(92\)90308-M](https://doi.org/10.1016/0045-7949(92)90308-M).
- [25] Hu X, Zhang R, Ren X, Pan C, Zhang X, Li H. Simplified design method for structure with viscous damper based on the specified damping distribution pattern. *J Earthq Eng* 2020:1–21.
- [26] Ingle RK, Chore HS. Soil-structure interaction analysis of building frames- an overview. *J Struct Eng SERC* 2007;34(5):201–9.
- [27] Jabary RN, Madabhushi SPG. Structure-soil-structure interaction effects on structures retrofitted with tuned mass dampers. *Soil Dyn Earthq Eng* 2017;100:301–15. <https://doi.org/10.1016/j.soildyn.2017.05.017>.
- [28] Kamaludin PNC, Kassem MM, Farsangi EN, Nazri FM, Yamaguchi E. Seismic resilience evaluation of RC-MRFs equipped with passive damping devices. *Earthq Struct* 2020;18(3):391–405.
- [29] Khoshnoudian F, Behmanesh I. Evaluation of FEMA-440 for including soilstructure interaction. *J Earthq Eng Eng Vib* 2010;9:397–408. <https://doi.org/10.1007/s11803-010-0024-2>.
- [30] Khoshnoudian F, Ziaei R, Ayyobi P, Paytam F. Effects of nonlinear soil-structure interaction on the seismic response of structure-tmd systems subjected to near-field earthquakes. *Bull Earthq Eng* 2017;15:199–226. <https://doi.org/10.1007/s10518-016-9963-y>.
- [31] Kitada Y, Iguchi M. Model test on dynamic cross interaction of adjacent buildings in nuclear power plants-an outline and outcomes of the project. In: Presented at the 13th world conference on earthquake engineering, Vancouver, B.C., Canada; 2004.
- [32] Kitada Y, Hirotsu T, Iguchi M. Models test on dynamic structure-structure interaction of nuclear power plant buildings. *Nucl Eng Des* 1999;192(2–3):205–16. [https://doi.org/10.1016/S0029-5493\(99\)00109-0](https://doi.org/10.1016/S0029-5493(99)00109-0).
- [33] Lee IK, Brown PT. Structures and foundation interaction analysis. *J Struct Eng Divis ASCE* 1972;11:2413–31.
- [34] Lee IK, Harrison HB. Structures and foundation interaction theory, Proc. ASCE, 96, ST 2; 1970. 177–198.
- [35] Li PZ, Hou XY, Liu YM, Lu XL. Shaking table model tests on dynamic structure-soil-structure interaction during various excitations. Presented at the 15th world conference on earthquake engineering, Lisbon, Portugal; 2012.
- [36] Lu Y, Hajirasouliha I, Marshall AM. Performance-based seismic design of flexible-base multi-storey buildings considering soil-structure interaction. *Eng Struct* 2016;108:90–103.
- [37] Mason HB, Trombetta NW, Chen Z, Bray JD, Hutchinson TC, Kutter BL. Seismic soil-foundation-structure interaction observed in geotechnical centrifuge experiments. *Soil Dyn Earthq Eng* 2013;48:162–74. <https://doi.org/10.1016/j.soildyn.2013.01.014>.
- [38] Morris D. Interaction of continuous frames and soil media. *J Struct Divis* 92(5); 1966: 13–44.
- [39] Muria-Vila D, Taborda R, Zapata-Escobar A. Soil-structure Interaction effects in two instrumented tall buildings. 13th World Conference on earthquake engineering, Vancouver, B.C., Canada. Paper No. 1911; 2004.
- [40] Nazariofard E, Zahrai SM. Fuzzy control of asymmetric plan buildings with active tuned mass damper considering soil-structure interaction. *Soil Dyn Earthq Eng* 2017;115:838–52. <https://doi.org/10.1016/j.soildyn.2017.09.020>.
- [41] Nigdeli SM, Bektaş G. Optimum tuned mass dampers for structures at rock and soil sites. *Proc Appl Math Mech PAMM* 2014;14(1):209–10.
- [42] Pitilakis D, Dietz M, Wood DM, Clouteau D, Modaressi A. Numerical simulation of dynamic soil-structure interaction in shaking table testing. *J Soil Dyn Earthq Eng* 2008;28(6):453–67. <https://doi.org/10.1016/j.soildyn.2007.07.011>.

- [43] Sarcheshmehpour M, Estekanchi HE, Ghannad MA. Optimum placement of supplementary viscous dampers for seismic rehabilitation of steel frames considering soil–structure interaction. *Struct Des Tall Special Build* 2020;29(1):e1682.
- [44] Sonmez M, Aydın E, Karabork T. Using an artificial bee colony algorithm for the optimal placement of viscous dampers in planar building frames. *Struct Multidiscip Optim* 2013;48:395–409. <https://doi.org/10.1007/s00158-013-0892-y>.
- [45] Shukla AK, Datta TK. Optimal use of viscoelastic dampers in building frames for seismic force. *J Struct Eng* 1999;125(4):401–9. [https://doi.org/10.1061/\(ASCE\)0733-9445\(1999\)125:4\(401\)](https://doi.org/10.1061/(ASCE)0733-9445(1999)125:4(401)).
- [46] Stewart JP, Fenves GL, Seed RB. Seismic soil-structure interaction in buildings. I: analytical aspects. *J Geotech Geoenviron Eng ASCE* 1999;125(1):26–37. [https://doi.org/10.1061/\(ASCE\)1090-0241\(1999\)125:1\(26\)](https://doi.org/10.1061/(ASCE)1090-0241(1999)125:1(26)).
- [47] Stewart JP, Seed RB, Fenves GL. Seismic soil-structure interaction in buildings II: empirical findings. *J Geotech Geoenviron Eng ASCE* 1999;125(1):38–48. [https://doi.org/10.1061/\(ASCE\)1090-0241\(1999\)125:1\(38\)](https://doi.org/10.1061/(ASCE)1090-0241(1999)125:1(38)).
- [48] Takewaki I. Optimal damper placement for minimum transfer functions. *Earthq Eng Struct Dyn* 1997;26:1113–24. [https://doi.org/10.1002/\(SICI\)1096-9845\(199711\)26:11<1113::AID-EQE696>3.0.CO;2-X](https://doi.org/10.1002/(SICI)1096-9845(199711)26:11<1113::AID-EQE696>3.0.CO;2-X).
- [49] Takewaki I. Soil-structure random response reduction via TMD-VD simultaneous use. *Comput Methods Appl Mech Eng* 2000;190(5–7):677–90. [https://doi.org/10.1016/S0045-7825\(99\)00434-X](https://doi.org/10.1016/S0045-7825(99)00434-X).
- [50] Takewaki I. Probabilistic critical excitation for MDOF elastic-plastic structures on compliant ground. *Earthq Eng Struct Dyn* 2001;30(9):1345–60. <https://doi.org/10.1002/eqe.66>.
- [51] Trombetta NW, Hutchinson TC, Mason HB, Zupan JD, Bray JD, Bolisetti C, et al. Centrifuge modelling of structure–soil–structure interaction: seismic performance of inelastic building models. In: Presented at the 15th world conference on earthquake engineering, Lisbon, Portugal; 2012.
- [52] Trombetta NW, Mason HB, Chen Z, Hutchinson TC, Bray JD, Kutter BL. Nonlinear dynamic foundation and frame structure response observed in geotechnical centrifuge experiments. *Soil Dyn Earthq Eng* 2013;50:117–33. <https://doi.org/10.1016/j.soildyn.2013.02.010>.
- [53] Tsuji M, Nakamura T. Optimum viscous dampers for stiffness design of shear buildings. *Struct Des Tall Special Build* 1996;5(3):217–34. [https://doi.org/10.1002/\(SICI\)1099-1794\(199609\)5:3<217::AID-TAL70>3.0.CO;2-R](https://doi.org/10.1002/(SICI)1099-1794(199609)5:3<217::AID-TAL70>3.0.CO;2-R).
- [54] Uz M, Hadi MNS. Optimal design of semi active control for adjacent buildings connected by MR damper based on integrated fuzzy logic and multi-objective genetic algorithm. *Eng Struct* 2014;69:135–48. <https://doi.org/10.1016/j.engstruct.2014.03.006>.
- [55] Wolfram Research. *Mathematica Edition, Version 5.0*. Champaign, Illinois: Wolfram Research; 2003.
- [56] Xiong W, Jiang LZ, Li YZ. Influence of soil–structure interaction (structure-to-soil relative stiffness and mass ratio) on the fundamental period of buildings: experimental observation and analytical verification. *Bull Earthq Eng* 2016;14:139–60. <https://doi.org/10.1007/s10518-015-9814-2>.
- [57] Xuefei Z, Shuguang W, Dongsheng DD, Weiqing L. Optimal design of viscoelastic dampers in frame structures considering soil-structure interaction effect. Article ID: 9629083 *Shock Vib* 2017. <https://doi.org/10.1155/2017/9629083>.
- [58] Xuefei Z, Shuguang W, Dongsheng D, Weiqing L. Simplified analysis of frame structures with viscoelastic dampers considering the effect of soil-structure interaction. *Earthq Eng Eng Vib* 2017;16:199–217. <https://doi.org/10.1007/s11803-017-0377-x>.
- [59] Yano T, Kitada Y, Iguchi M, Hirotsu T, Yoshida K. Model test on dynamic cross interaction of adjacent buildings in nuclear power plants. In: Presented at the 12th world conference on earthquake engineering, New Zealand; 2000.
- [60] Yano T, Naito Y, Iwamoto K, Kitada Y, Iguchi M. Model test on dynamic cross interaction of adjacent building in nuclear power plants overall evaluation on field test. In: Presented at the 17th international conference on structural mechanics in reactor technology, Prague; 2003.
- [61] Zhang RH, Soong TT. Seismic design of visco-elastic dampers for structural applications. *Struct Eng ASCE* 1992;118(5):1375–92. [https://doi.org/10.1061/\(ASCE\)0733-9445\(1992\)118:5\(1375\)](https://doi.org/10.1061/(ASCE)0733-9445(1992)118:5(1375)).
- [62] Zhang RH, Soong TT, Mahmoodi P. Seismic response of steel frame structures with added viscoelastic dampers. *Earthq Eng Struct Dyn* 1989;18(3):389–96. <https://doi.org/10.1002/eqe.4290180307>.